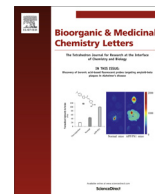




Contents lists available at ScienceDirect

# Bioorganic & Medicinal Chemistry Letters

journal homepage: [www.elsevier.com/locate/bmcl](http://www.elsevier.com/locate/bmcl)

## Carbon nanodots as molecular scaffolds for development of antimicrobial agents



Maria Ngu-Schwemlein<sup>a,\*</sup>, Suk Fun Chin<sup>b</sup>, Ryan Hileman<sup>a</sup>, Chris Drozdowski<sup>a</sup>, Clint Upchurch<sup>a</sup>, April Hargrove<sup>a</sup>

<sup>a</sup> Department of Chemistry, Winston-Salem State University, Winston-Salem, NC 27110, USA

<sup>b</sup> Department of Chemistry, Universiti Malaysia Sarawak, 94300 Kota Samarahan, Sarawak, Malaysia

### ARTICLE INFO

#### Article history:

Received 28 December 2015

Revised 16 February 2016

Accepted 17 February 2016

Available online 18 February 2016

#### Keywords:

Carbon nanodots

PAMAM

Molecular scaffold

Antimicrobial activities

Synergism

### ABSTRACT

We report the potential of carbon nanodots (CNDs) as a molecular scaffold for enhancing the antimicrobial activities of small dendritic poly(amidoamines) (PAMAM). Carbon nanodots prepared from sago starch are readily functionalized with PAMAM by using *N*-ethyl-*N'*-(3-dimethylaminopropyl)carbodiimide hydrochloride (EDC) and *N*-hydroxysuccinimide (NHS). Electron microscopy images of these polyaminated CNDs show that they are approximately 30–60 nm in diameter. Infrared and fluorescence spectroscopy analyses of the water-soluble material established the presence of the polyamidoaminated moiety and the intrinsic fluorescence of the nanodots. The polyaminated nanodots (**CND-PAM1** and **CND-PAM2**) exhibit in vitro antimicrobial properties, not only to non-multidrug resistant bacteria but also to the corresponding Gram-negative multidrug bacteria. Their minimum inhibitory concentration (MIC) ranges from 8 to 64 µg/mL, which is much lower than that of PAMAM G1 or the non-active PAMAM G0 and CNDs. Additionally, they show synergistic effect in combination with tetracycline or colistin. These preliminary results imply that CNDs can serve as a promising scaffold for facilitating the rational design of antimicrobial materials for combating the ever-increasing threat of antibiotic resistance. Moreover, their fluorescence could be pertinent to unraveling their mode of action for imaging or diagnostic applications.

© 2016 Elsevier Ltd. All rights reserved.

The ever-increasing incidence of bacterial resistance to existing antibiotics has created a need to broaden the targets as well as to develop new antimicrobials and strategies to combat antibiotic resistant bacteria.<sup>1,2</sup> Carbon nanodots (CNDs) are a fascinating new class of nanomaterials that are promising molecular templates for various different types of applications including imaging, sensing, drug delivery, photocatalysis, and more.<sup>3–6</sup> They are readily prepared from starch and other carbonaceous sources<sup>7–9</sup> and their low toxicity index promises numerous biomedical applications besides their fluorescent properties.<sup>10,11</sup>

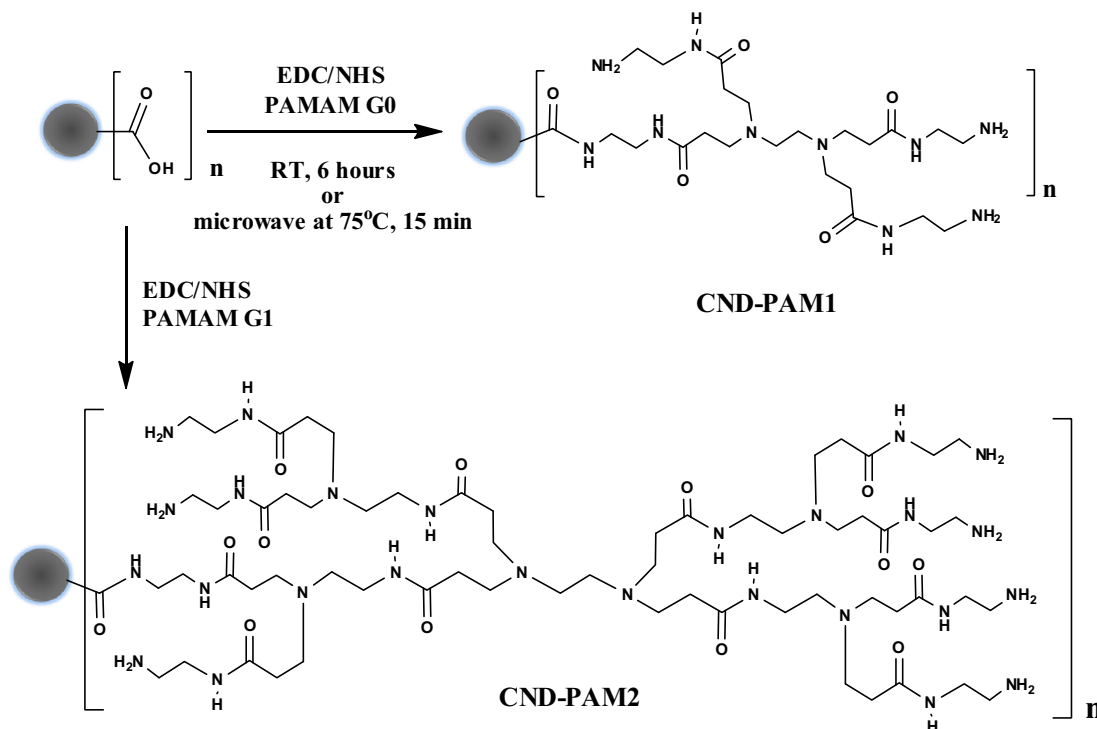
Carbon nanodots, like their nanotube congeners, offer reactive surface functional groups that can be oxidized by acid reflux to generate carboxylic acid containing dots.<sup>8,12–14</sup> Such surface decorated functional moieties on the carbon dots allowed for further passivation, with various compounds such as *N*-acetyl-cysteine, PEG<sub>1500</sub>N, and other polymers, to improve their fluorescence properties.<sup>15–17</sup> Accordingly, CNDs could serve as a molecular scaffold

for grafting small polycationic amines. The nanoscale carbon dots offer high surface areas suited for concentrating such cationic densities for enhanced antimicrobial activity. Structurally large polycationic compounds including poly-lysines, cationic amphipathic peptides, and large polyamine dendrimers have been reported to exert antimicrobial activities. They disrupt the integrity of bacterial membranes, which possess an overall net anionic charge, via favorable electrostatic and hydrophobic interactions.<sup>18–20</sup> Moreover, some of these polycationic compounds enhanced the uptake of small hydrophobic antibiotics into the bacterium, and consequently, presented synergistic effects. For example, an alpha-helical cationic peptide was reported to exert a potent synergistic effect with chloramphenicol against some types of bacteria.<sup>21</sup>

Poly(amidoamines) (PAMAM) dendrimers consist of an interior ethylene diamine core surrounded by successive branching layers (generations) that terminate with amino groups.<sup>20,22</sup> Although the higher generation PAMAM dendrimers (greater than generation three, G3) exhibit antibacterial properties, the flexible and open lower generation dendrimers lacks significant efficacy.<sup>20</sup> Therefore, we explore carbon nanodots as a molecular scaffold

\* Corresponding author. Tel.: +1 336 750 2919; fax: +1 336 750 2549.

E-mail address: [Schwemleinmn@wssu.edu](mailto:Schwemleinmn@wssu.edu) (M. Ngu-Schwemlein).



**Scheme 1.** Polyaminated carbon nanodots conjugated with PAMAM generation G0 and G1.

for conjugating these lower generation PAMAM (G0 and G1) to concentrate their aminated cationic densities and hence, assess these conjugates for enhanced antimicrobial activity. Dendritic PAMAMs expressing primary amino groups are readily utilized for conjugation onto the surface carboxylated CNDs. Some common conjugation approaches in dendrimer engineering include their nucleophilic acyl substitution reaction with *N*-hydroxysuccinimide (NHS) activated carboxylic acids or *N*-ethyl-*N'*-(3-dimethylaminopropyl)carbodiimide hydrochloride (EDC) and *N*-hydroxybenzotriazole (HOBt) coupling chemistry.<sup>23,24</sup>

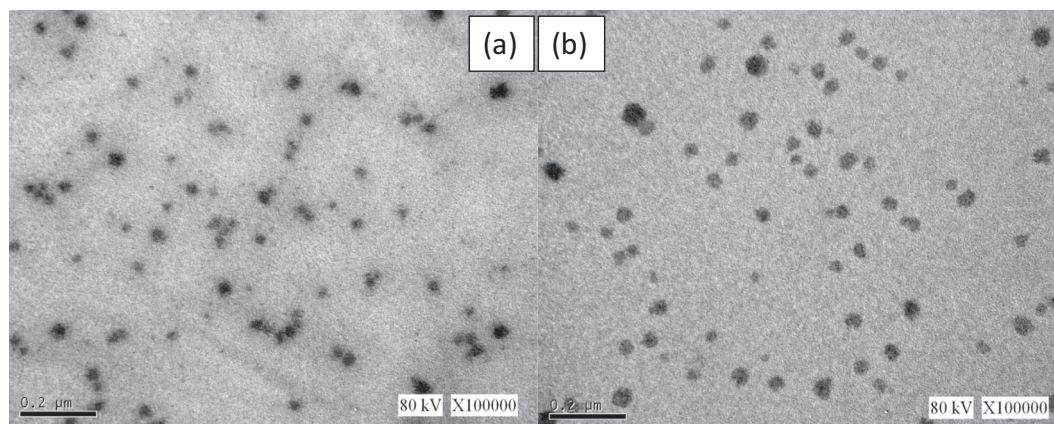
The preparation of conjugated CND and PAMAMs were realized using the previously reported surface oxidized CNDs,<sup>25</sup> via an amidation reaction by EDC and NHS activations of the carboxyl carbon toward nucleophilic acyl substitution (**CND-PAM1** and **CND-PAM2**, Scheme 1).

The syntheses was achieved in one-step by either stirring at room temperature for 5–6 h or under microwave irradiation at 60 W for 10–15 min with a maximum temperature of 75 °C (see Supplementary data). The water-soluble excess EDC, NHS, and salts

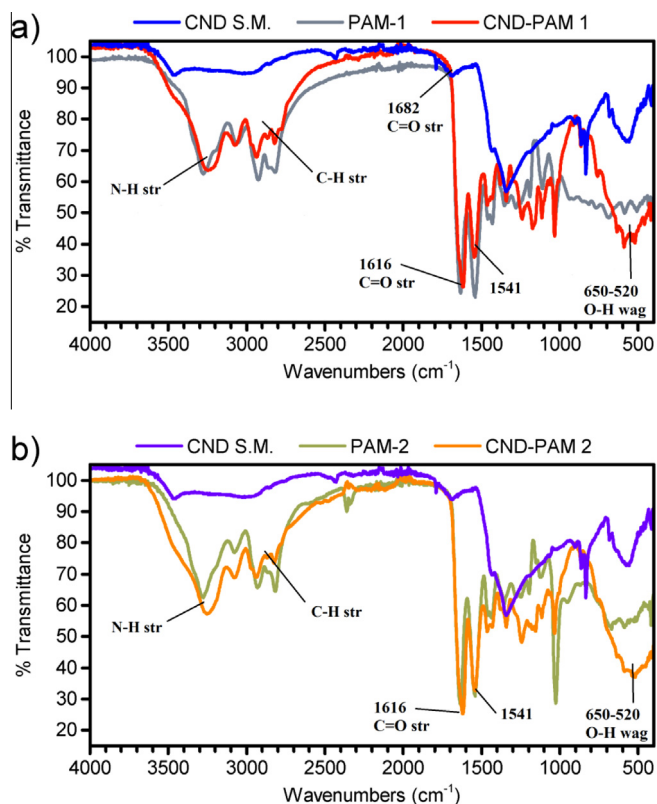
were readily removed by dialysis and their separation was monitored by size exclusion HPLC. Both **CND-PAM1** and **CND-PAM2** were obtained as yellowish brown powder following lyophilization. The morphology of **CND-PAM2** is slightly larger than **CND-PAM1** and their diameter size ranges from 30 to 60 nm (Fig. 1). Both conjugates were also characterized using infrared, fluorescence and ultraviolet spectroscopy as discussed below.

Figure 2a shows the infrared spectra of the polyamidoaminated CND (**CND-PAM1**), CND, and PAMAM G0 (PAM-1). **CND-PAM1** shows characteristic absorption bands of surface functional groups, for example, there are stretching vibrations of N–H at 3100–3600 cm<sup>−1</sup>, C–H at 3000–2800 cm<sup>−1</sup>, and bending vibrations of CH<sub>2</sub> 1350–1460 cm<sup>−1</sup>. The amide I band (C=O stretching) occurs at 1616 cm<sup>−1</sup> and the amide II band, resulting from the interaction of N–H bending and the C–N stretching of the C–N–H groups, is observed at 1541 cm<sup>−1</sup>, as previously reported.<sup>26</sup>

Similarly, **CND-PAM2** exhibits absorption bands corresponding to the polyamidoaminated CND (**CND-PAM2**), CND, and PAMAM G1 (PAM-2). Both **CND-PAM1** and **CND-PAM2** show most of the



**Figure 1.** Transmission electron microscope (TEM) images of (a) **CND-PAM1** and (b) **CND-PAM2**.



**Figure 2.** Fourier transformed Infrared spectra of starting material CND (CND S.M.) and PAMAM compared with (a) **CND-PAM1** and (b) **CND-PAM2**.

IR absorption bands that are present in their corresponding PAMAM precursor and the O–H out-of-plane bending absorption band ( $650\text{--}520\text{ cm}^{-1}$ ), which is characteristic of the hydroxyl-rich starch derived CND precursor (Fig. 2a and b). The above-observed cues of functional groups present in the CND and PAMAM conjugates, in contrast to that recorded for the CND precursor; demonstrate that the PAMAM dendrimer are linked to the CND molecular framework.

Strong fluorescence emission was observed for the polyaminated CNDs at a range of  $420\text{--}460\text{ nm}$  when the excitation wavelength is between  $330\text{ and }350\text{ nm}$  (Fig. 3). These results are consistent with those reported for the starting material<sup>25</sup> except for a  $10\text{ nm}$  red shift observed in the emission maximum peak for **CND-PAM1** to  $440\text{ nm}$  (Fig. 3a). Additionally, the fluorescence peak for **CND-PAM1** is broader than that observed for **CND-PAM2**

**Table 1**

Antimicrobial susceptibility test results<sup>a</sup>

Bacteria	CND-PAM1 <sup>c</sup> ( $\mu\text{g/mL}$ )	CND-PAM2 ( $\mu\text{g/mL}$ )
<i>E. coli</i> 25922	8	8
<i>S. aureus</i> 10566	32	32
<i>K. pneumonia</i> 13883	32	64
<i>K. pneumonia</i> 1706 <sup>b</sup>	8	16
<i>P. aeruginosa</i> 27853	8	16
<i>P. aeruginosa</i> 1744 <sup>b</sup>	8	16
<i>A. baumannii</i> 1605 <sup>b</sup>	8	16

<sup>a</sup> MIC values were derived from at least three independent experiments.

<sup>b</sup> Antibiotic resistant strains.

<sup>c</sup> CND, PAMAM G0, and their non-conjugated mixtures did not exhibit any antimicrobial activities. PAMAM G1 showed an MIC of  $64\text{ }\mu\text{g/mL}$  against *E. coli*, but no activity against *S. aureus* at  $512\text{ }\mu\text{g/mL}$ .

(Fig. 3b). The latter could be attributed to a larger variation in the polyamination of CND by the structurally smaller PAMAM G0 compared to the larger PAMAM G1.

The dried powdery polyaminated CNDs were evaluated for antimicrobial activity by following the antimicrobial susceptibility testing standards. The precursors of the conjugates including CND, PAMAM G0, PAMAM G1, and equal mixtures of CND and PAMAMs were also examined for comparison. Table 1 shows the MIC values ( $\mu\text{g/mL}$ ), the minimum concentration of the test compound necessary to inhibit detectable bacterial growth at  $620\text{ nm}$ . The data shows promising MICs for both polyaminated CNDs, but no significant antimicrobial activities were observed for the controls and non-conjugated mixtures of CND and PAMAMs. Both polyaminated CNDs exhibited the same activity against representative Gram-negative (*Escherichia coli*) and -positive (*Staphylococcus aureus*) bacteria (Table 1). However, they show a fourfold selectivity for *E. coli* at an MIC of  $8\text{ }\mu\text{g/mL}$ . Accordingly, they were subsequently tested against three prioritized Gram-negatives from the “ESKAPE” pathogens (*Enterococcus faecium*, *Staphylococcus aureus*, *Klebsiella pneumoniae*, *Acinetobacter baumannii*, *Pseudomonas aeruginosa*, and *Enterobacter* species) that are categorized by the US Center for Disease and Control as urgent or serious because they are responsible for two thirds of all health care-associated infections.<sup>2</sup>

MIC results show that the antimicrobial activities of these surface polyaminated CND scaffold are effective against both antibiotic resistant (*K. pneumonia* 1706, *P. aeruginosa* 1744, and *A. baumannii* 1605) and non-resistant strains (*K. pneumonia* 13883, *P. aeruginosa* 27853). Remarkably, they are fourfold more effective in killing the resistant *K. pneumonia* strain than the corresponding non-resistant strain. This suggests that the resistant strain may be more vulnerable to these compounds regardless of the degree of polycationization. However, **CND-PAM1** is consistently twice as

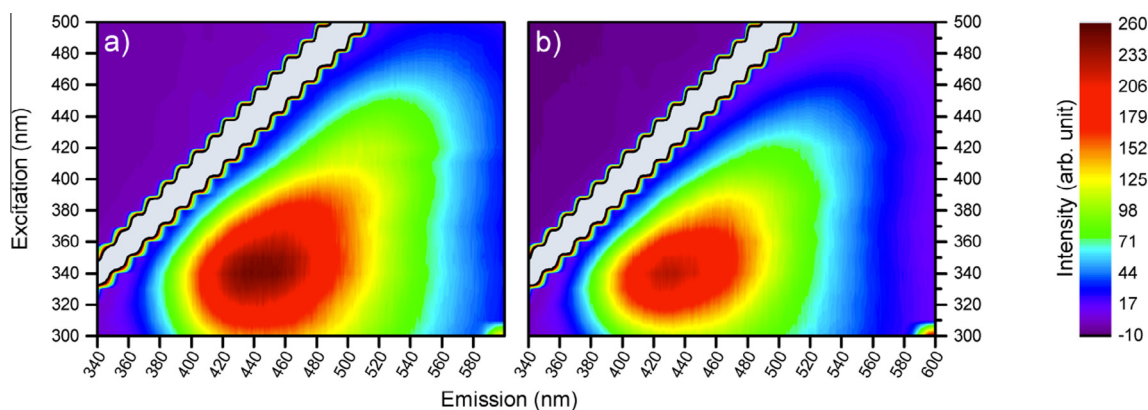


**Figure 3.** Fluorescence emission contour plot showing excitation wavelength ranging from  $340\text{ to }600\text{ nm}$  for (a) **CND-PAM1**, and (b) **CND-PAM2**.

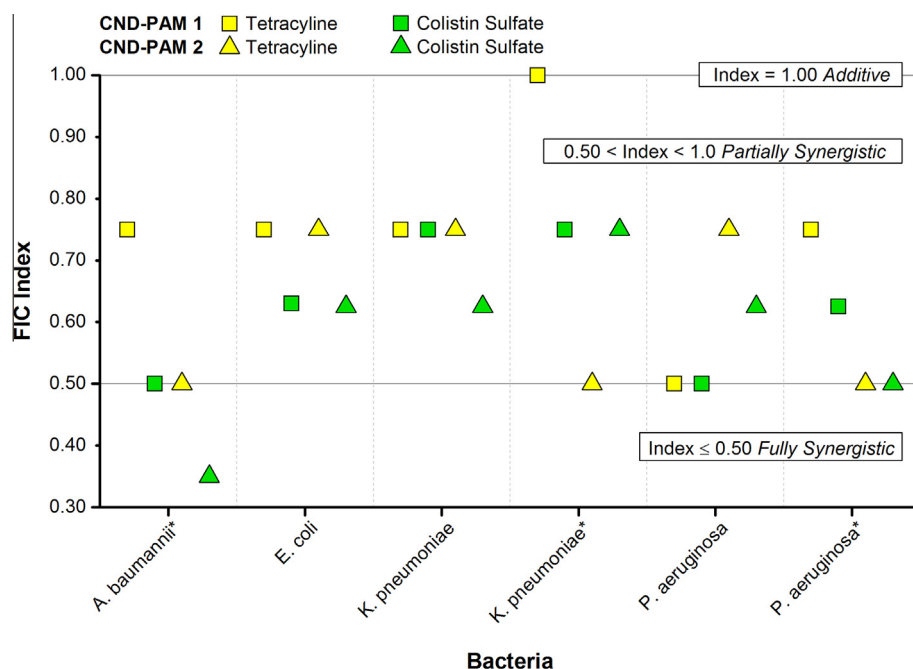


**Figure 4.** Comparison of FIC indices for synergism between **CND-PAM1** and **CND-PAM2** with tetracycline or colistin against various bacteria where \* denotes antibiotic resistant strains.

active as **CND-PAM2** against the select Gram-negative bacteria suggesting that CND functionalized with smaller dendrimeric amines maybe more effective against Gram-negatives. Notably, each polyaminated CND type exhibits the same MIC value against *P. aeruginosa* 27853, *P. aeruginosa* 1744 (resistant strain), and *A. baumannii* 1605 (resistant strain), suggesting that a threshold in antimicrobial activity may have been reached by each polycationized CND.

In general, the antimicrobial activity and selectivity of **CND-PAM1** and **CND-PAM2** are similar (MIC values range from 8 to 32 µg/mL), and are comparable to those reported for outer-membrane cell wall disrupting amphipathic  $\alpha$ -helical peptides through detergent-like action.<sup>27,28</sup> This suggests that CNDs could be useful as a molecular scaffold for grafting small polycationic amines to enhance their antimicrobial activities by increasing their cationic densities for optimal interactions with the polyanionic outer surface of the bacterial membrane. Such electrostatic perturbation could result in bacterial membrane-disruptive effects that could assist in the simultaneous uptake of small hydrophobic antibiotics and thereby impart synergistic antimicrobial effects. Accordingly, we evaluated them for in vitro synergism in combination with tetracycline, an antibiotic commonly used to treat pneumonia, acne, and urinary tract infections, and colistin, an antibiotic of last therapeutic option for infections caused by multi-drug resistant (MDR) 'superbugs'. Checkerboard titration assay<sup>29</sup> was conducted to measure the interaction between the conjugates and antibiotics in an in vitro bacterial culture to determine whether they acted in synergy to increase killing efficiency. This combination assay provides a numerical value calculated as a fractional inhibition concentration (FIC) index by measuring the effective MIC for the combined test compounds. Accordingly, an FIC index of 0.5 corresponds to a 4-fold decrease in the MIC of each test compound in combination constitutes synergism.

As shown in Figure 4, both **CND-PAM1** and **CND-PAM2** in combination with tetracycline or colistin exhibited some variations in partial synergistic antimicrobial activity ( $FIC > 0.5$  and  $< 1$ ). However, tetracycline and **CND-PAM1** showed an additive effect ( $FIC = 1$ ) against the resistant strain *K. pneumonia*, whereas colistin

and **CND-PAM2** exhibited a greater than fourfold increase in activity ( $FIC = 0.35$ ) against *A. baumannii* (see Supplemental section). In general, the multi-drug resistant *A. baumannii* is more vulnerable to the combination treatment as observed by the associated lower FIC indexes (Fig. 4). The majority of these polyaminated CNDs exhibited partial synergism with tetracycline and colistin, independent of bacterial type. This is consistent with synergism displayed by polycationic peptides, which are attributed to their detergent-like mode of action on the bacterial membrane. Similarly, the polycationic CNDs could disrupt the integrity of bacterial membrane, resulting in enhanced antibiotic uptake and faster inhibition of bacterial growth.

In conclusion, we have reported the use of CNDs as an effective molecular scaffold for conjugating small dendritic poly(amidoamines)s to increase their antimicrobial efficacy. Moreover, these poly(amidoamines) functionalized CNDs in combination with tetracycline or colistin show improved antimicrobial activities. Overall, the results obtained from this study indicate that CNDs can serve as a promising molecular scaffold for the conjugation of dendritic polyamines that can be used as synergists or carriers for small hydrophobic antibiotics to enhance their uptake and hence increase antibacterial action. Moreover, the intrinsic fluorescence properties of CNDs could be useful for optimizing the rational design of targeted antimicrobial combination therapy with select antibiotics.

## Acknowledgments

This work was partially supported by the NIH NIGMS (SC3GM088134), and an AAAS WIRC MIs grant. S.-F. Chin acknowledges support from FRGS/STG05(01)/960/2013(01).

## Supplementary data

Supplementary data (preparation and experimental procedures, spectroscopic data, and numerical FIC data) associated with this article can be found, in the online version, at <http://dx.doi.org/10.1016/j.bmcl.2016.05.011>.



1016/j.bmcl.2016.02.047. These data include MOL files and InChI-Keys of the most important compounds described in this article.

## References and notes

- World Health Organization *Antimicrobial Resistance: Global Report on Surveillance*; WHO Press: Geneva, Switzerland, 2014. URL: <<http://www.who.int/drugresistance/documents>> Accessed on 12/20/2015.
- Centers for Disease Control and Prevention *Antibiotic Resistance Threats in the United States*, 2013. URL: <<http://www.cdc.gov/drugresistance/threat-report-2013/pdf>> Accessed on 12/20/2015.
- Ding, H.; Du, F.; Liu, P.; Chen, Z.; Shen, J. *Appl. Mater. Interfaces* **2015**, *7*, 6889.
- Thakur, M.; Pandey, S.; Mewada, A.; Patil, V.; Khade, M.; Goshi, E.; Sharon, M. J. *Drug Delivery* **2014**. <http://dx.doi.org/10.1155/2014/282193> 282193.
- Ding, C.; Zhu, A.; Tian, Y. *Acc. Chem. Res.* **2014**, *47*, 20.
- Wang, W.; Chemg, L.; Liu, W. G. *Sci. China B* **2014**, *1*.
- Li, H.; Kang, Z.; Liu, Y.; Lee, S.-T. *J. Mater. Chem.* **2012**, *22*, 24230.
- Peng, H.; Travas-Sejdic, J. *Chem. Mater.* **2009**, *21*, 5563.
- Wang, Q.; Zheng, H.; Long, Y.; Zhang, L.; Gao, M.; Bai, W. *Carbon* **2011**, *49*, 3134.
- Roy, P.; Chen, P.-C.; Periasamy, A. P.; Chen, Y.-N.; Chang, H.-T. *Mater. Today* **2015**, *18*, 447.
- Yang, S.-T.; Wang, X.; Wang, H.; Lu, F.; Luo, P. G.; Cao, L.; Meziani, M. J.; Liu, J.-H.; Liu, Y.; Chen, M.; Huang, Y.; Sun, Y.-P. *J. Phys. Chem. C* **2009**, *113*, 18110.
- Liu, J.; Lin, L.; Wang, X.; Lin, S.; Cai, W.; Zhang, L.; Zheng, Z. *Analyst* **2012**, *137*, 2637.
- Murugan, E.; Vimala, G. J. *Colloid Interface Sci.* **2011**, *357*, 354.
- Zardinia, H. Z.; Amirib, A.; Shanbedib, M.; Maghrebib, M.; Baniadamb, M. *Colloids Surf. B* **2012**, *92*, 196.
- Goncalves, H.; Jorge, P. A. S.; Fernades, J. R. A.; Esteves da Silva, J. C. G. *Sens. Actuators, B* **2010**, *145*, 702.
- Sun, Y.-P.; Zhou, B.; Lin, Y.; Wang, W.; Shiral Fernando, K. A.; Pathak, P.; Harruff, B. A.; Wang, X.; Wang, H.; Luo, P. G.; Yang, H.; Chen, B.; Veca, L. M.; Xie, S.-Y. *J. Am. Chem. Soc.* **2006**, *128*, 7756.
- Dong, Y.; Wang, R.; Li, G.; Chen, C.; Chi, Y.; Chen, G. *Anal. Chem.* **2012**, *84*, 6220.
- Hancock, R. E. W.; Rozek, A. *FEMS Microbiol. Lett.* **2002**, *206*, 143.
- Li, Y.-Q.; Han, Q.; Feng, J.-L.; Tian, W.-L.; Mo, H.-Z. *Food Control* **2014**, *43*, 22.
- Calabretta, M. K.; Kumar, A.; McDermott, A. M.; Cai, C. *Biomacromolecules* **2007**, *8*, 1807.
- Park, Y.; Park, S. N.; Park, S. C.; Shin, S. O.; Kim, J. Y.; Kang, S. J.; Kim, M. H.; Jeong, C. Y.; Hahm, K. S. *Biochim. Biophys. Acta* **2006**, *764*, 24.
- Malik, N.; Wiwattanapatapee, R.; Klopsch, R.; Lorenz, K.; Frey, H.; Weener, J. W.; Meijer, E. W.; Paulus, W.; Duncan, R. J. *Control Release* **2000**, *65*, 133.
- Wu, L.-P.; Ficker, M.; Christensen, J. B.; Trohopoulos, P. N.; Moghimi, S. M. *Bioconjugate Chem.* **2015**, *26*, 1198.
- Durán-Lara, E.; Guzmán, L.; John, A.; Fuentes, E.; Alarcón, M.; Palomo, I.; Santos, L. S. *Eur. J. Med. Chem.* **2013**, *69*, 601.
- Chin, S.-F.; Akmar, S.; Pang, S. C.; Ng, S. M. *Mater. Lett.* **2012**, *85*, 50.
- Amiri, A.; Zardini, H. Z.; Shanbedi, M.; Maghrebi, M.; Baniadam, M.; Tolueinia, B. *Mater. Lett.* **2012**, *72*, 153.
- Legrand, B.; Laurencin, M.; Sarkis, J.; Duval, E.; Mouret, L.; Hubert, J.-F.; Collen, M.; Vie, V.; Zatylny-Gaudin, C.; Henry, J.; Baudy-Floc'h, M.; Bondon, A. *Biochim. Biophys. Acta* **2011**, *1808*, 106.
- Ngu-Schwemlein, M.; Dumond, J.; Rudd, L.; Rigaud, J.-H. *Aust. J. Chem.* **2015**, *68*, 218.
- Jeong, N.; Kim, J. Y.; Park, S. C.; Lee, J. K.; Gopal, R.; Yoo, S.; Son, B. K.; Hahm, J. S.; Park, Y.; Hahm, K. S. *Biochem. Biophys. Res. Commun.* **2010**, *399*, 581.